

Three Cycles of the Solar Toroidal Magnetic Field and This Peculiar Minimum

LO, Leyan, HOEKSEMA, J.T. and SCHERRER, P.H.

HEPL, Stanford University, Stanford, CA 94305-4085, USA

Abstract. Thirty-four years of WSO (Wilcox Solar Observatory) and thirteen years of SOHO/MDI (Michelson Doppler Imager on the Solar and Heliospheric Observatory) magnetograms have been studied to measure the east-west inclination angle, indicating the toroidal component of the photospheric magnetic field. This analysis reveals that the large-scale toroidal component of the global magnetic field is antisymmetric around the equator and reverses direction in regions associated with flux from one solar cycle compared to the next. The toroidal field revealed the first early signs of cycle 24 at high latitudes, especially in the northern hemisphere, appearing as far back as 2003 in the WSO data and 2004 in MDI. As in previous cycles, the feature moves gradually equatorward. Cycles overlap and the pattern associated with each cycle lasts about 17 years. Even though the polar field at the current solar minimum is significantly lower than the three previous minima, the toroidal field pattern is similar.

1. Introduction

Solar dynamo models predict that the toroidal and poloidal components of the global magnetic field are regenerated from one other. The poloidal field is transformed into the toroidal field from differential rotation (the Ω -effect), and the toroidal field is twisted into the poloidal field (the α -effect). These alternate and repeat in a 22 year cycle [e.g. Dikpati et al., 2008].

This toroidal field component, previously measured by Shrauner & Scherrer [1994] using WSO data over the period of 1977-1992, provided evidence for an extended activity cycle of 16-18 years. Ulrich & Boyden [2005] also measured the toroidal field using Mount Wilson data from 1986-2004 and verified the dynamo model for the creation and reversal of the toroidal field.

Since we are facing a peculiar solar minimum, we want to investigate whether there is also some peculiar activity in the toroidal fields leading up to the minimum. Three solar cycles of WSO magnetic field data are available to us now, as well as a complete cycle observed with SOHO/MDI [Scherrer et al., 1995].

2. Method & Results

We first generated maps of the inclination angle for both the positive and negative field polarities using the WSO magnetograms and the MDI synoptic maps. This is done by tracking the line-of-sight magnetic field, B_l , for a given Carrington coordinate as it crosses the disk. We can fit the measurements of B_l for different longitudes to the following equation to calculate the average east-west

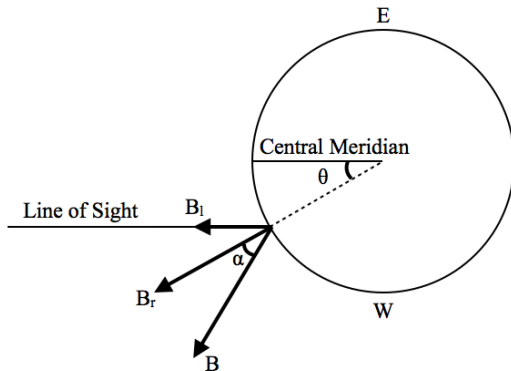


Figure 1. Diagram of the field components and angles as viewed from the north pole. The east-west field inclination angle, α , is the angle between B and B_r . We measure B_l as it crosses the disk over various θ 's.

inclination angle of the field, α :

$$B_l(\theta) = A \cos(\theta + \alpha) \quad (1)$$

Where A is proportional to the true magnetic field. A derivation of this fit gives the following formula (Shrauner & Scherrer, 1994):

$$\tan \alpha = \frac{(\sum_i B_l^i \cos \theta_i)(\sum_i \sin \theta_i \cos \theta_i) - (\sum_i B_l^i \sin \theta_i)(\sum_i \cos^2 \theta_i)}{(\sum_i B_l^i \cos \theta_i)(\sum_i \sin^2 \theta_i) - (\sum_i B_l^i \sin \theta_i)(\sum_i \sin \theta_i \cos \theta_i)} \quad (2)$$

We fit the values of B_l and θ into the equation for α to generate maps of the inclination angles. Following Shrauner & Scherrer, individual regions are tracked across the WSO magnetograms. For MDI, measurements of the same features in synoptic maps constructed using data from central meridian, $\pm 15^\circ$, $\pm 30^\circ$ and $\pm 45^\circ$ are compared. We generate two separate maps for each Carrington rotation, one for positive polarity B_l and the other for negative. The difference of these two maps gives the inclination difference. This inclination difference map gives us the east-west direction of the magnetic field at each point on the sun for each Carrington rotation.

The inclination difference maps for each rotation are averaged over all longitudes to show the inclination differences at each latitude over time, using both WSO and MDI data. From these averages we construct the contour plots shown in Figure 2, and the line plots (Figure 3) for each hemisphere. The WSO data span 34 years, which gives us three solar cycles of coverage.

However, the MDI values are somewhat different than WSO, as can be seen in Figure 4. We believe this is due to asymmetric noise characteristics of the MDI instrument. In 2003, SOHO began to periodically roll from 0° to 180° , which caused periodic irregularities in our data that need to be better calibrated.

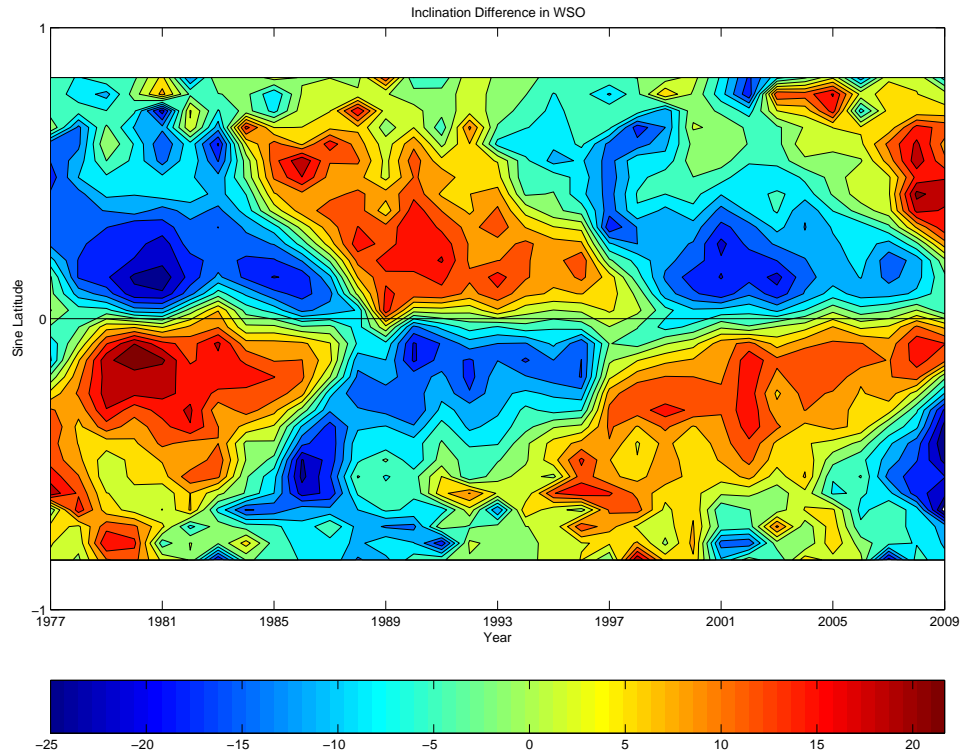


Figure 2. Contour plot of the rotation averages of inclination differences versus latitude from 1977-2009 using WSO data. There are almost three complete cycles of inclination differences, and the extended solar minimum can be seen in both the duration of cycle 23 near the equator, as well as in the rate at which cycle 24 moves equatorward. Toroidal field associated with Cycle 24 first emerges in 2003 in the north at high latitudes and the pattern looks almost identical to the last two cycles.

3. Summary

From the inclination difference summary averages, we detected the first emergence of Cycle 24 some time during 2003-2004. This emergence pattern is very much like the pattern observed in the previous two cycles. The new emerging inclination angles, which are related to the toroidal fields, are consistent with those from the previous cycles. This suggests that the toroidal field is not a clear indicator of the duration of the following solar minimum or the generation of the poloidal fields at the concurrent minimum. However, if the toroidal field is generated from the preceding poloidal field, we might expect to see that the next cycle's toroidal field will be weak. Also, the inclination angle that indicates the toroidal field at the Sun's surface is only a distant reflection of the toroidal field that is present wherever the true solar dynamo is acting. Particularly in the higher resolution MDI data, the weak field regions that contribute to the analysis may also reflect the spatially averaged characteristics of a surface dynamo process whose contribution to the solar cycle dynamo is uncertain. Further work needs to be done to solve the calibration issues of MDI.

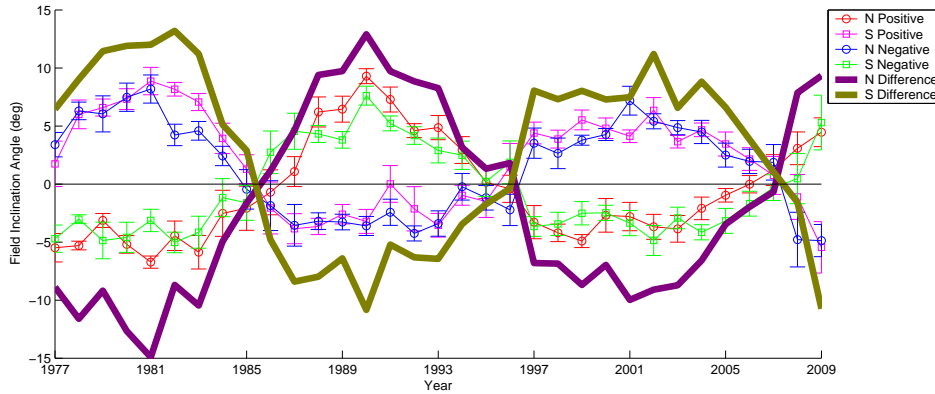


Figure 3. Line plot of the summary averages of WSO inclinations for each hemisphere from 1977-2009. The lighter lines show each polarity separately. The heavy red (green) line shows the inclination difference in the north (south). In 2007, the average northern and southern field angles flip sign, indicating the start of Cycle 24. The sign changes when most of the weak field regions in each hemisphere have reversed their toroidal field components. Oddly enough, the extended minimum is not observed in the line plot; the interval between zero crossings this cycle is the same as last.

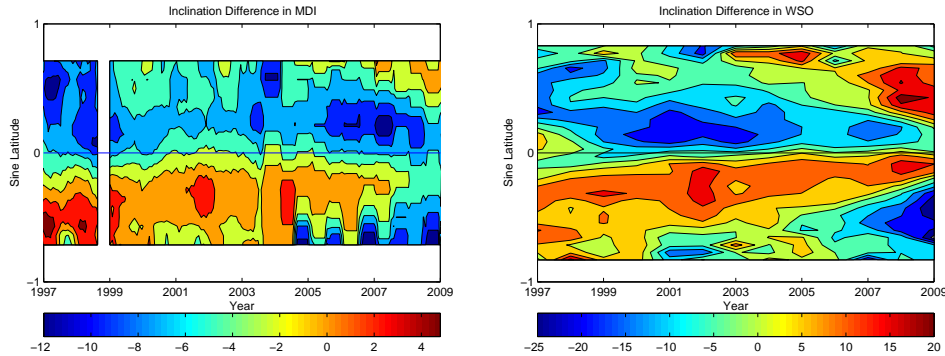


Figure 4. The plot generated from MDI (left) span only one cycle, from 1997-2009. The general shape of the contour map matches WSO's for this time period (right). Both MDI and WSO show an extended Cycle 23 and the emergence of Cycle 24 in 2004 in the north at high latitudes. Periodic rolls of the spacecraft after 2003 add noise to MDI.

Acknowledgments. This work was supported by NASA under MDI Grant NNX09AI90G and WSO Grant NNX08AG47G. SOHO is a project of international cooperation between ESA and NASA.

References

- Dikpati, M., de Toma, G. & Gilman, P.A.; 2008, *Ap.J.*, 675 920.
 Scherrer, P.H., et al.; 1995, *Sol. Phys.*, 162, 129.
 Shrauner, J. A., & Scherrer, P. H.; 1994, *Sol. Phys.*, 153, 131.
 Ulrich, R. K., & Boyden, J. E.; 2005, *Ap.J.*, 620, 123.